Journal of Hazardous Materials 175 (2010) 216–223

Contents lists available at ScienceDirect

Journal of Hazardous Materials

journal homepage: www.elsevier.com/locate/jhazmat

Adsorption of Ba^{2+} by Ca-exchange clinoptilolite tuff and montmorillonite clay

M.L. Chávez[a,*], L. de Pablo[b,2], T.A. García[a,1]

[a] Facultad de Química, Universidad Nacional Autónoma de México, Cd. Universitaria, 04510 México, D. F., Mexico
[b] Instituto de Geología, Universidad Nacional Autónoma de México, Cd. Universitaria, 04510 México, D. F., Mexico

ARTICLE INFO

Article history:
Received 2 March 2009
Received in revised form 13 August 2009
Accepted 30 September 2009
Available online 20 October 2009

Keywords:
Clinoptilolite
Montmorillonite
Barium adsorption

ABSTRACT

The adsorption of barium by Ca-exchanged clinoptilolite and montmorillonite is presented. The kinetics of adsorption of Ba^{2+} were evaluated contacting 1 g portion of each adsorber with 100 mL 0.1N $BaCl_2$ for 200 h. Adsorption by Ca-clinoptilolite is defined by second-order kinetics of rate constant K_v 8.232×10^{-2} g mg^{-1} h^{-1} and maximum removal of 71.885 mg g^{-1}. It is a two-stage process initiated by a rapid uptake of Ba^{2+} followed by more moderate kinetics. The adsorption isotherms were determined contacting 0.2 g of each adsorber with 10 mL 0.1–0.005N $BaCl_2 + CaCl_2$ solution, Ba^{2+}/Ca^{2+} ratio 1, for periods of 7 days for the tuff and 2 days for the clay. The equilibrium adsorption is described by the Langmuir model, of equilibrium constant K 0.0151 L mg^{-1} and maximum adsorption of 15.29 mg g^{-1}. The adsorption of Ba^{2+} by Ca-exchanged montmorillonite also follows a second-order reaction of rate constant K_v 3.179×10^{-2} g mg^{-1} h^{-1}, and calculated separation of 36.74 mg g^{-1}; the Langmuir isotherm is defined by the constant K 0.034 L mg^{-1} and maximum adsorption of 15.29 mg g^{-1}. X-ray diffraction shows that the exchange of Ba^{2+} modifies the d_{001} of Ca-montmorillonite from 15.4 to 12.4 Å.

1. Introduction

Adsorption has been established as an effective and economical technology to concentrate and remove contaminants from aqueous phases and soils. In the process, contaminants are separated from the aqueous phase and immobilized in the adsorbent from which they can safely be disposed or recovered [1–3]. Among the preferred adsorbers are natural clays and zeolites which are usually considered by their low cost, ample distribution and preference for specific contaminants [4–6].

The crystal structure and characteristics of clays and zeolites are well-established and are not further discussion. As a general comment, both mineral groups are crystalline aluminosilicates formed by SiO_4 and AlO_4 tetrahedra and octahedra sharing oxygen atoms to form three-dimensional structural networks [7,8]. In the zeolite minerals the structural arrangements develop channels through which ions pass through or are adsorbed, retained or exchanged according with the characteristics and dimensions of channels and ions, hence defining the suitability of the zeolite for specific adsorptions [7]. Among the most common zeolites is clinoptilolite, which has been applied in its natural state or modified by HCl and NaCl treatments to the removal of Cr^{3+}, Cu^{2+}, Cd^{2+}, Hg^{2+}, Zn^{2+}, Ni^{2+} and Pb^{2+} [8–16]. In the clay minerals, rings of SiO_4 and AlO_4 tetrahedra share oxygen atoms with $Al(OH)O_4$ octahedra to develop layered structures with internal active surfaces and edges on which ions are adsorbed. Often, the interlayer spaces of clays could be more suitable to separate larger and more complex ions than the internal channels of zeolites [17]. Adsorption and immobilization of cations by smectites, specifically by montmorillonite, has been analyzed in recent years by Bhattacharyya and Gupta [3], including the immobilization of Pb^{2+}, Cd^{2+} and Ni^{2+} on dehydroxylated montmorillonite [2,18], of Cd^{2+}, Co^{2+}, Cu^{2+}, Pb^{2+} and Ni^{2+} by acid-activated montmorillonite [3,19], and of Cu^{2+}, Pb^{2+} and Zn^{2+} exchanged with Ca-montmorillonite [20].

Barium is a contaminant that has been largely ignored, especially regarding its adsorption by zeolites and clays. Its adsorption from aqueous solutions by Na-clinoptilolite was considered by Blanchard et al. [21] and Faghihian et al. [22], who found it to be of the same order than lead; more recent studies on Italian zeolites indicated that barium is only successfully exchanged by Na-phillipsite and Na-chabazite [1,23]. The adsorption of Ba^{2+} by montmorillonite was studied by Eylem et al. [24] and by Na-montmorillonite by several authors [25–27]. No further work has been published on the adsorption of barium by zeolite minerals, specifically clinoptilolite, or by clay minerals of the montmorillonite or smectite types.

Abbreviations: Cln, clinoptilolite tuff; Ca-Cln, Ca-exchanged clinoptilolite tuff; Ba-Cln, Ba-exchanged clinoptilolite tuff; Mnt, montmorillonite clay; Ca-Mnt, Ca-exchanged montmorillonite clay; Ba-Mnt, Ba-exchanged montmorillonite clay.

* Corresponding author. Tel.: +52 56223505; fax: +52 56223531.
E-mail addresses: marilu@servidor.unam.mx, marilulilit@hotmail.com (M.L. Chávez), liberto@servidor.unam.mx (L. de Pablo), nenaquim@hotmail.com, nenaquim@gmail.com (T.A. García).
[1] Tel: +52 56223505; fax: +52 56223531.
[2] Tel: +52 56224285x132.

0304-3894/$ – see front matter © 2009 Elsevier B.V. All rights reserved.
doi:10.1016/j.jhazmat.2009.09.151

Contamination by Ba^{2+} is associated with natural and industrial sources, including waste from oil paint pigments like barium chloride [28], nuclear waste [29,30], drilling oil and gas industry [31], and barite mining [30,32–34]; barium is often associated with arsenic in ground waters [35]. It has been employed as a Ra^{2+} analog (ion radii Ba^{2+} 1.34, Ra^{2+} 1.43) in the study of interactions of nuclear contaminants [26]. Barium sulfate usually used for contrast radiography of the digestive tract is an extremely insoluble salt of low toxicity but the concentration of Ba^{2+} in hospital waste and sewage sludge from some treatment plants has been found as high as 1.58 mg g^{-1} [36]. In México, abnormal Ba^{2+} concentrations of 0.0073–0.0101 mg g^{-1} have been recognized in mining areas in the vicinity of Avalos, Chihuahua, M. Benavides, Nuevo Casas Grandes and Ojinaga [32], and in old painted roofs and building interiors in Sonora [37]. Some barium compounds dissolve easily and are found in lakes, rivers and streams. The toxicity of barium is related to its solubility and for insoluble salts increases with decreasing pH. The EPA (US Environmental Protection Agency) [38] allows a maximum of 0.002 mg g^{-1} of Ba in drinking water. The harmful effects of ingesting low levels of Ba^{2+} over long periods has not been established [33,36]; however, soluble salts of barium have proved to be harmful to animals, plants and humans [39–42]. High concentrations of Ba^{2+} have been associated with multiple sclerosis and neurodegenerative diseases [39]. Generally speaking, accumulation of heavy metals in the environment represents serious threat to human health, living resources and ecological systems [9,14].

Our present interest is on the adsorption of barium by clinoptilolite tuff and by montmorillonite clay in their calcium exchanged forms. The Ca-saturated minerals were selected because of the preferred accumulation of Ca^{2+} in some soils and waters and even in waste dumps; by incorporating Ca^{2+} to the systems we attempt to approximate natural environmental conditions where Ca^{2+} rather than Na^{+} is predominant, hence departing from adsorption studies performed on pure or Na-exchanged mineral zeolites and clays.

2. Experimental

2.1. Materials

Clinoptilolite is found in extensive deposits of volcanoclastics in southern México, where occurs associated with heulandite and mordenite [43,44]. Also located are suitable deposits of bentonite and smectite [45,46]. The clinoptilolite tuff (Cln) used in the following studies was from Laollaga, Oaxaca, in southern México [47,48]. The geology of the area and mineralogy of the tuff had been described [43,44,48,49]. The tuff is constituted by clinoptilolite-heulandite and mordenite with minor plagioclase, feldspar, cristobalite, quartz and glass; its cation exchange capacity is of 1.2 mequiv. g^{-1}, and clinoptilolite represents ~60% of the tuff. The montmorillonite clay (Mnt) is from Cuencamé, Durango, contains ~85% montmorillonite associated with plagioclase, feldspar, glass, opal and calcite, and has a cation exchange capacity of 0.64 mequiv. g^{-1} [45,46]. It was selected essentially for its purity in preference to less pure comparable clays occurring in locations closer to Laollaga, Oaxaca [50].

2.2. Methodology

Clinoptilolite tuff and montmorillonite clay were analyzed prior to and after the adsorption experiments by X-ray diffraction (XRD), thermal differential and thermogravimetric analysis (DTA, TGA) and by infrared spectroscopy (IR). The diffraction studies were performed on a SIEMENS D5000 diffractometer using Ni-filtered CuKα radiation, range 2–60°2θ, step size 0.02°2θ, counting time 3 s. Thermal DTA and TGA were carried in a TGA/SDTA Mettler Toledo 851E analyzer, air flow, heating rate 10 °C/min, range 25–800 °C. IR spectroscopy was performed in a Bruker Vector 22 FTIR, range 4000–400 cm^{-1}, samples pressed at 350 kg/cm^2 into KBr disks. Chemical analysis of Ba^{2+} and Ca^{2+} was determined by atomic absorption spectrometry (AAS) using a Varian Espectra A220 unit, acetylene-nitrous oxide flame, Ba^{2+} absorption wavelength 553.6 nm, capillary flow 5 mL min^{-1}, and 0.01% of 20,000 ppm KCl solution was added as ionization suppressor.

Reagent exchange solutions were prepared from analytical-grade $BaCl_2{\cdot}2H_2O$ and $CaCl_2{\cdot}2H_2O$ dissolved in deionized water. Ca-saturated clinoptilolite tuff (Ca-Cln) and montmorillonite clay (Ca-Mnt) were prepared by grinding to 0.075 mm particle size and reacting 10 g portions with 450 mL 1N $CaCl_2$, 24 h, decanting thrice in succession, and finally washing with deionized water until total removal of Cl^- as detected by $AgNO_3$. Both adsorbers were afterwards kept at 60 °C for 3 days before final light crushing to pass the 1 mm screen and be retained on the 0.075 mm screen.

The kinetics of adsorption of Ba^{2+} by Ca-exchanged clinoptilolite and Ca-exchanged montmorillonite clay were evaluated by contacting 1 g portion of each adsorber with 100 mL 0.1N $BaCl_2$ for 200 h, taking 0.25 mL aliquots after 1, 2, 3, 4, 5, 10, 20, 60, 120, 180 and 200 h contact time and analyzing them by Ba^{2+}. Aliquots taken from the clay required centrifuging at 3400 rpm for 5 min to separate suspended material. The solid residues after reaction were washed until Cl^- free ($AgNO_3$ test) and analyzed by XRD, IR and DTA.

The adsorption isotherms or time to establish steady-state conditions were determined by contacting 0.2 g of each Ca-exchanged adsorber with 10 mL $BaCl_2 + CaCl_2$ solution of variable concentration 0.1, 0.05, 0.025, 0.020, 0.015, 0.010 and 0.005N, Ba^{2+}/Ca^{2+} ratio 1, for periods of 7 days for the tuff and 2 days for the clay. After reaction, the decanted or centrifuged liquids were analyzed for Ba^{2+} and Ca^{2+} by AAS. By using dual $Ba^{2+} + Ca^{2+}$ solutions it was intended to evaluate the adsorption behavior of Ba^{2+} from Ca-rich liquids and any resultant mutual interference on the sorption process.

2.3. Adsorption model

The kinetics of adsorption was calculated from the second-order reaction [51] (Eq. (1))

$$\frac{dq_t}{dt} = K_v(q_e - q_t)^2 \quad (1)$$

where K_v (g mg^{-1} h^{-1}) is the second-order rate constant of adsorption, q_e (mg g^{-1}) the amount of Ba^{2+} adsorbed at equilibrium and q_t (mg g^{-1}) the Ba^{2+} on the adsorbent at any time t. At boundary conditions t varies between 0–t and q_t between 0–q_t, hence the integrated equation takes the form of Eq. (2) where $K_v q_e^2$ is the initial adsorption rate. The linear variation of t/q_t vs. t allowed calculation of q_e and K_v. The validity of the assumed order of reaction and calculated equation was tested by comparison of calculated and experimental q_e [2].

$$\frac{t}{q_t} = \frac{1}{K_v q_e^2} + \frac{1}{q_e}t \quad (2)$$

The Ba^{2+} adsorbed by the mineral was calculated from mass-balance equation (3)

$$Q_e M = V(C_0 - C_e) \quad (3)$$

where Q_e is the final concentration of Ba^{2+} in the adsorber (mg g^{-1}), C_0 the initial concentration of Ba^{2+} (mg L^{-1}), C_e the final concentration of Ba^{2+} in solution (mg L^{-1}), M the adsorber mass (g) and V the volume of liquid (L). The adsorption equilibrium is described by the isotherm equation whose parameters correspond to the surface properties and affinity of the adsorbent; it is usually the Langmuir isotherm which assumes that cation uptake on the homogeneous

Table 1
Chemical composition of clinoptilolite tuff and montmorillonite clay[a].

	Clinoptilolite tuff	Montmorillonite clay
SiO_2	68.30	60.96
TiO_2	0.21	0.07
Al_2O_3	11.79	14.49
FeO	1.83	1.34
MgO	0.05	5.28
CaO	1.68	0.74
Na_2O	3.22	1.62
K_2O	2.39	0.55
H_2O^-		8.77
H_2O^+		5.87
LOI[a]	10.48	8.77
Clinoptilolite	60	
Montmorillonite		85
Opal	10	
Plagioclase	7	5
Quartz		5
K-feldspar	3	3
Glass	20	
Glass, calcite		2
CEC[a]	120	64
Na	61	7
Ca	36	32
Mg	3	24
K	20	1

[a] Analysis in wt%, LOI loss of ignition, CEC cation exchange capacity in mequiv./100 g.

surface of the adsorber is by sorption of monolayers without interaction between adsorbate and adsorber, on uniformly distributed adsorption sites. The linear form of the Langmuir isotherm is represented by Eq. (4)

$$\frac{1}{Q_e} = \frac{1}{b} + \frac{1}{(bK)C_e} \quad (4)$$

where Q_e is the Ba^{2+} adsorbed at equilibrium ($mg\,g^{-1}$), C_e the equilibrium concentration of adsorbate ($mg\,L^{-1}$), K ($L\,mg^{-1}$) and b ($mg\,g^{-1}$) the Langmuir constants related to adsorption energy and maximum adsorption capacity. The slope and intercept to the origin of plotting $1/Q_e$ vs. $1/C_e$ represent the Langmuir parameters of Eq. (4) [52].

3. Results and discussion

3.1. Materials characterization

The composition and cation exchange characteristics of the tuff and clay are presented in Table 1. X-ray diffraction profiles of clinoptilolite tuff and montmorillonite clay in their natural, Ca- and Ba-exchanged forms indicate that the zeolite fraction of the tuff is composed of major clinoptilolite-heulandite and minor mordenite (Fig. 1). Exchanging the tuff with calcium and barium to produce Ca-Cln and Ba-Cln does not displace the 0 2 0 clinoptilolite reflection from its characteristic 8.95 Å spacing. The diffraction profiles of montmorillonite show that calcium and barium exchange modify the hydration state of montmorillonite and the d_{001} spacing (Fig. 2); in the process, 14.6 Å natural montmorillonite changes to 15.4 Å montmorillonite when exchanged with Ca^{2+} (Ca-Mnt) which in turn transforms to 12.4 Å montmorillonite when Ca^{2+} is exchanged by Ba^{2+} (Ba-Mnt); Cases et al. [53] have shown that homoionic montmorillonite develops two-layer hydrates when exchanged with Ca^{2+}, Mg^{2+} and Sr^{2+} and one-layer hydrate when Ba^{2+} is the adsorbate.

Thermal characterization by DTA and TGA in the range from room temperature to 350 °C (Fig. 3, Table 2) shows that both natural tuff and clay dehydrate at 100–105 °C with losses of 4.84 and

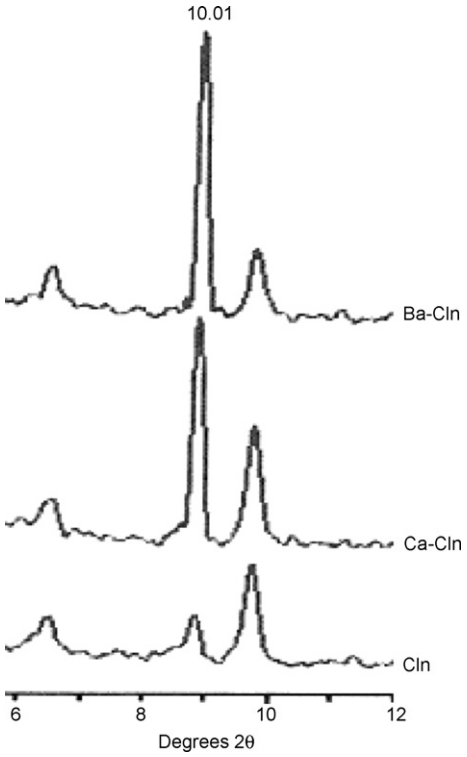

Fig. 1. X-ray diffraction profiles in the 6–12°2θ range of (a) clinoptilolite tuff, (b) Ca-exchanged tuff, and (c) Ba-exchanged tuff. The clinoptilolite d_{020} reflection at 10.01 Å changes intensity with Ca^{2+} and Ba^{2+} exchange.

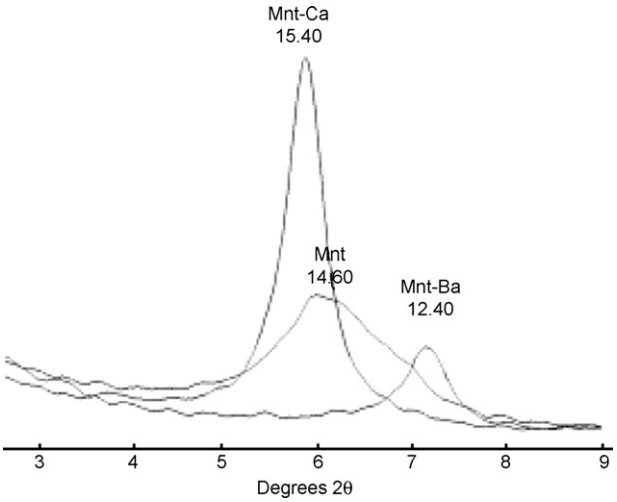

Fig. 2. X-ray diffraction profile in the 3–9°2θ range of (a) montmorillonite clay, (b) Ca-exchanged clay, and (c) Ba-exchanged clay. Variations in d_{010} correspond to different stages of hydration resulting from cation adsorption and displacement.

Table 2
Thermal behavior of clinoptilolite tuff and montmorillonite clay.

	Dehydration temperature		Weight loss
Clinoptilolite tuff	105		4.84
Ca-exchanged clinoptilolite	113	58	6.12
Ba-exchanged clinoptilolite	117	60	6.65
Montmorillonite clay	100		1.87
Ca-exchanged montmorillonite	150	86	5.55
Ba-exchanged montmorillonite	125	80	5.10

Dehydration temperature in °C, weight loss in wt%.

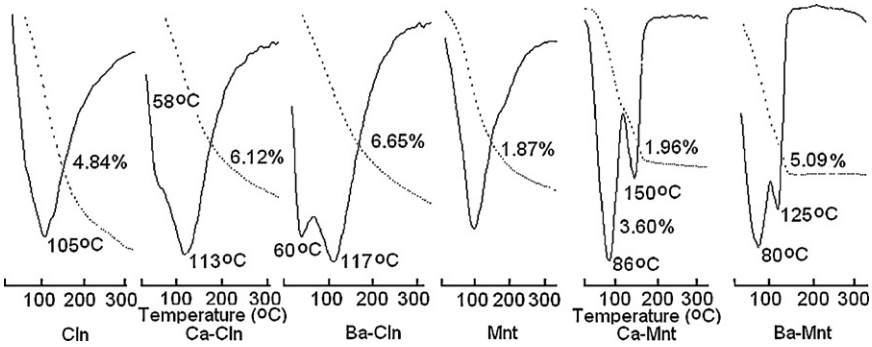

Fig. 3. Thermal profiles of clinoptilolite tuff and montmorillonite clay in the room temperature – 350 °C range. The tuff adsorbs more water than the clay; cation adsorption increases dehydration temperatures and adsorbed water.

1.87 wt% water. Adsorption of calcium by the tuff develops a second endotherm at 58 °C owing to weakly bound H_2O molecules, displaces the intense dehydration caused by more strongly held H_2O molecules to 113 °C and increases the overall zeolite water to 6.12 wt%. Exchange of calcium by barium moves reactions to 60 and 117 °C while raising the zeolitic water to 6.65 wt%. In the montmorillonite clay, adsorption of calcium results in an endothermic reaction at 86 °C equally caused by weakly bound H_2O molecules, movement of the second reaction to 150 °C and increases of overall water to 5.55 wt%; exchange by barium moves the dehydration temperatures to 80 and 125 °C and the water to 5.10 wt%. Hence, adsorption of cations forms hydrates of low-interaction energy and weakly bound H_2O molecules and hydrates of greater thermal stability bound to non-framework cations possibly located on less accessible sites [54].

Infrared absorption profiles show similar spectra for Ca-Cln and Ca-Mnt (Fig. 4, Table 3). There are only minor differences in the absorbance of the ~3624 cm^{-1} band owing to surface hydroxyls Si–OH–Si and Al–OH–Al which are higher in montmorillonite and Ba-exchanged montmorillonite, in the octahedral AlAl(OH) 918 cm^{-1} band from the clay and the T–O bonds of both minerals.

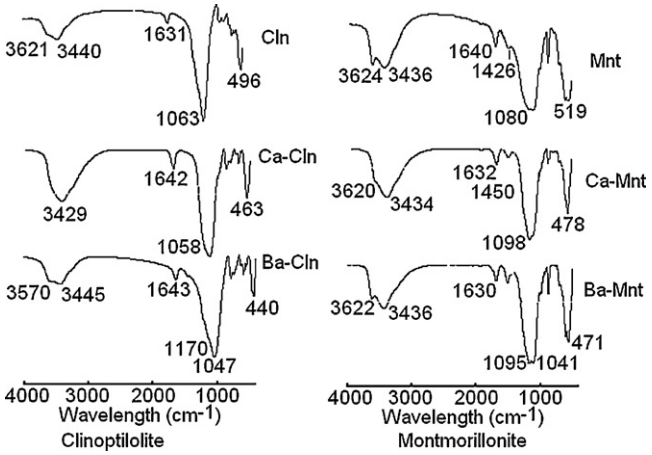

Fig. 4. Infrared absorption profiles of clinoptilolite tuff and montmorillonite clay. Main differences reside in the octahedral AlAl(OH) bond showed by the clay and the tetrahedral T–O bond shown by both minerals.

3.2. Adsorption kinetics and equilibrium

3.2.1. Kinetics

Adsorption of Ba^{2+} by Ca-Cln and by Ca-Mnt is in both cases a two-stage process comprising an initial fast intake of Ba^{2+} lasting nearly 60 min followed by a much slower adsorption that is essentially completed and attains equilibrium after 10 h of contact. The Ca-exchanged clinoptilolite tuff adsorbs Ba^{2+} with 83.53% efficiency after 60 min contact, which rises to 95.13% efficiency after 10 h (Fig. 5) there remaining a neglected 4.87%. The Ca-exchanged montmorillonite clay adsorbs Ba^{2+} with an efficiency of 23.33% after 60 min which increases to 94.33% after 10 h (Fig. 5). Hence, Ca-clinoptilolite is in short runs a faster and more efficient barium adsorber than Ca-montmorillonite.

The kinetics of adsorption was examined as first-order and second-order kinetic models. A satisfactory fit between calculated and experimental data indicated that the exchange of Ba^{2+} by Ca-Cln is a second-order reaction kinetics ($R^2 = 0.9999$) of rate constant K_v 8.232×10^{-2} g mg^{-1} h^{-1} and calculated maximum adsorption q_e of 71.885 mg g^{-1} (1.047 mequiv. g^{-1}) (Fig. 6, Table 4). The kinetics of adsorption by Ca-Mnt is similarly described by a second-order reaction of rate constant K_v 3.179×10^{-2} g mg^{-1} h^{-1} and calculated maximum adsorption of 36.743 mg g^{-1} (0.535 mequiv. g^{-1}) (Fig. 6, Table 4).

3.2.2. Equilibrium

The equilibrium adsorption of Ba^{2+} by Ca-Cln indicates that Ba^{2+} enrichment is accompanied by Ca^{2+} depletion and is described by the Langmuir equation (Eq. (5)) and corresponding isotherm (Fig. 7) of constant K estimated at 0.015 L mg^{-1}

Table 3
Infrared absorption spectra of clinoptilolite tuff and montmorillonite clay natural, Ca- and Ba-exchanged.

Clinoptilolite			Montmorillonite			Band[a]
3621	–	3670	3624	3620	3622	Si–OH–Si, Al–OH–Al
3440	3428	3440	3436	3434	3436	H–O–H stretching
1631	1642	1642	1640	1632	1630	H–O–H bending
1063	1068	1078	1080	1088	1095	Si–O–Si(Al) stretching
–	–	–	918	918	918	AlAl–OH
793	797	797	796	796	795	Si–O–Si(Al) stretching
601	591	690	–	–	–	Si–O–Si(Al) bending
496	463	440	469	478	471	T–O bending

[a] Band position in cm^{-1}.

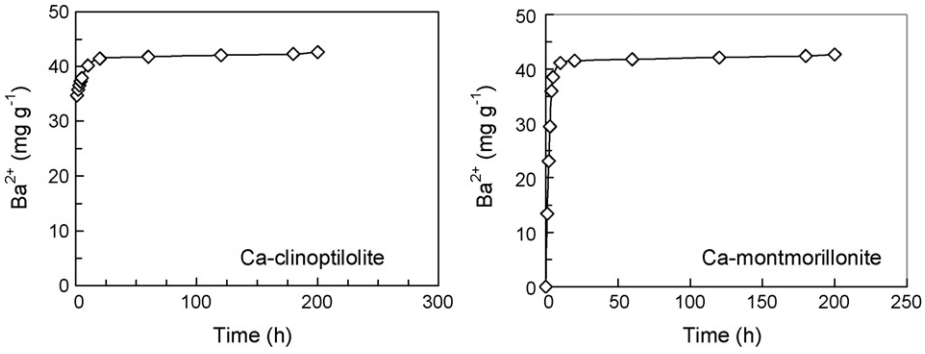

Fig. 5. Variation of the Ba^{2+} adsorbed by Ca-exchanged clinoptilolite tuff and montmorillonite clay.

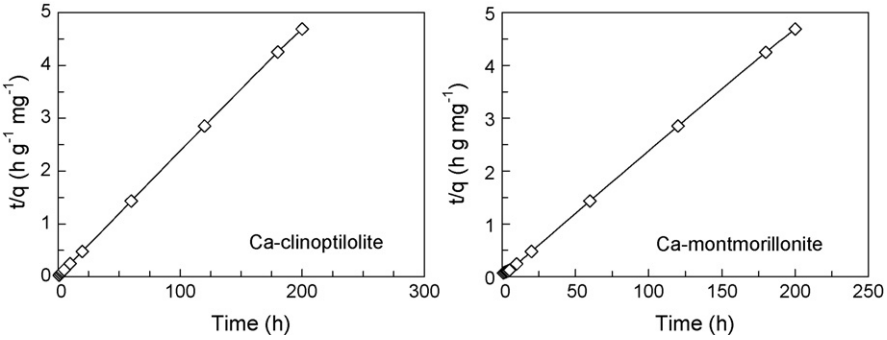

Fig. 6. Second-order kinetics for the adsorption of Ba^{2+} by Ca-exchanged clinoptilolite tuff and montmorillonite clay.

Table 4
Kinetics and Langmuir parameters for the Ba^{2+} adsorption by Ca-exchanged clinoptilolite tuff and montmorillonite clay.

	Ca-exchanged	
	Cln	Mnt
Kinetics of adsorption		
$K_v \times 10^2$ [a]	8.232	3.179
q_e	71.885	36.743
R^2	0.9999	0.9999
Adsorption equilibrium		
K	0.015	0.034
b	15.29	15.29
R	1	1

[a] Units K_v (g mg^{-1} h^{-1}), q_e (mg g^{-1}), K (L mg^{-1}), b (mg g^{-1}).

and maximum Ba^{2+} adsorption of 15.29 mg g^{-1} (0.22 mequiv. g^{-1}) (Table 4).

The equilibrium exchange of Ba^{2+} by Ca-Mnt shows similar correlation between Ba^{2+} enrichment and Ca^{2+} depletion from the clay. The adsorption data fit a Langmuir isotherm ($R = 1$) of constant K 0.034 L mg^{-1} and maximum adsorption b of 15.29 mg g^{-1} (0.22 mequiv. g^{-1}) (Fig. 7, Table 4) described by Eq. (6).

$$\frac{1}{Q_e} = 0.0654 + \frac{4.4414}{C_e} \quad (5)$$

$$\frac{1}{Q_e} = 0.0654 + \frac{1.8863}{C_e} \quad (6)$$

Adsorption of Ba^{2+} from $Ba^{2+} + Ca^{2+}$ solutions by Ca-exchanged clinoptilolite tuff and by Ca-exchanged montmorillonite clay is coupled with displacement of Ca^{2+} from the adsorber to the solution, described by the reaction

$$Ba_{(S)}{}^{2+} + Ca_{(C,M)}{}^{2+} \rightarrow Ba_{(C,M)}{}^{2+} + Ca_{(S)}{}^{2+} \quad (7)$$

In weak solutions, Ca^{2+} is rapidly released but as its concentration in the solution increases the Ca^{2+} retained by the adsorber tends towards constancy. In the clinoptilolite, inflexion occurred at a Ca^{2+} concentration of 16.8 mequiv. L^{-1} (336 mg g^{-1}) (Fig. 8) and in the clay inflexion was at 13.71 mequiv. L^{-1} (274 mg g^{-1}) (Fig. 8).

3.2.3. Discussion

The adsorption of Ba^{2+} by Ca-Cln is a two-stage process where variations in the adsorption can be broadly attributed to crystal

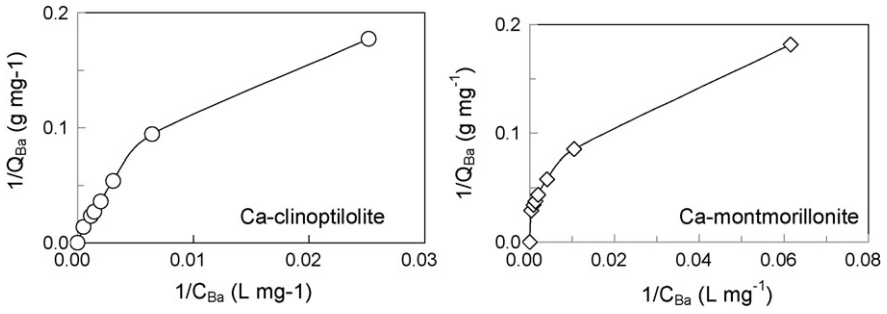

Fig. 7. Langmuir isotherms of the adsorption of Ba^{2+} by Ca-exchanged clinoptilolite tuff and Ca-exchange montmorillonite clay.

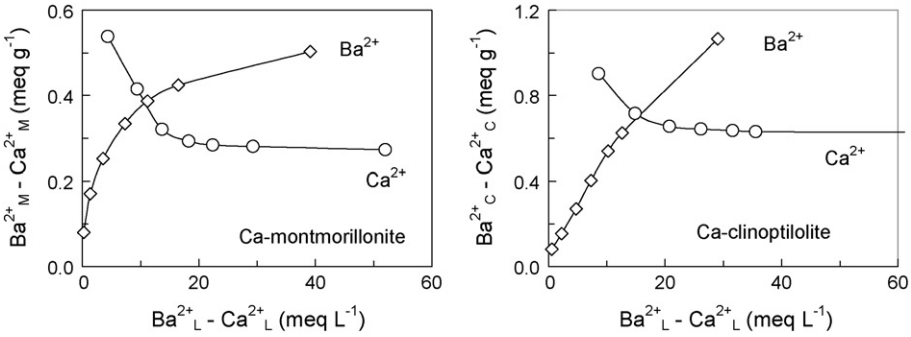

Fig. 8. Exchange isotherm of Ba^{2+} by Ca-exchanged clinoptilolite tuff and montmorillonite clay from Ba^{2+} + Ca^{2+} solutions. Data represents the concentration of Ba^{2+} and Ca^{2+} in the tuff or the clay vs. Ba^{2+} in the solution.

structure, size and shape of available sites and nature of the adsorbate. An applicable hypothesis attributes the initial rapid exchange of heavy metals by clinoptilolite to accommodation of exchanged cations in easily accessible sites while continuing slower exchange is associated with internal micropores of more difficult access [9].

Our data indicate that adsorption of Ca^{2+} by natural clinoptilolite tuff develops a low-interaction energy hydrate of H_2O molecules weakly bound to Ca^{2+}, thereby increasing the overall content of zeolitic water. Replacing Ca^{2+} by Ba^{2+} raises the number of H_2O molecules in a hydrate of nearly equal low-interaction energy, further augmenting the zeolitic water. Through adsorption, the second higher energy hydrate that characterizes the tuff increases its energy slightly while retaining essentially the same amount of H_2O. The adsorption of Ba^{2+} increases the surface hydroxyl activity, as indicated by the ~3640 cm^{-1} IR absorption band. Hence, thermal and IR data sustain formation of low-energy Ca^{2+} and Ba^{2+} hydrates weakly bound most probably on external sites where pH-sensitive protonation reactions proceed. Higher energy hydrates with non-framework Ca^{2+} and Ba^{2+} would accumulate on sites of more difficult access.

Barium in aqueous media can be in the forms of Ba^{2+}, $Ba(OH)_2$, $Ba^{2+}(H_2O)_n$ (n = 4–7), and $[Ba(H_2O)_6]^{2+}$. Barium hydrates average radius of 4.04 Å [55,56]. Clinoptilolite that has channel openings of 3.1 Å may adsorb Ba^{2+} but may find it difficult to adsorb hydrous ions of larger size, hence limiting the adsorption of hydrates $[Ba(H_2O)_n]^{2+}$ to species with $n > 6$ or to those hydrates where hydroxyls could be partially replaced by oxygens from the zeolite framework [55]. Montmorillonite can adsorb Ba^{2+} on the crystal edges and interlayer surface possibly at dissimilar rates, in the forms of low- and high-energy hydrates in outer- and inner-sphere surface complexes. Zhang et al. [26] concluded from X-ray absorption fine structure spectroscopy (XAFS) studies that a fraction of Ba^{2+} is adsorbed as inner-sphere surface complexes on the crystal edges of montmorillonite through sharing oxygens from de-protonated hydroxyls from aluminum octahedrons; the separations between Ba^{2+} and O^{2-} of the first shell and Ba^{2+} and Al^{3+} of the second shell are consistent with the geometry of inner-sphere complexes at the edge sites. Our studies indicate that exchange of Ca^{2+} by Ba^{2+} in Ca-Cln and Ca-Mnt is not totally accomplished, leaving residual Ca^{2+} in the adsorbers. In the clinoptilolite, adsorbed Ba^{2+} amounts to 0.63 mequiv. g^{-1}. In montmorillonite the adsorbed Ba^{2+} is 0.39 mequiv. g^{-1}.

Our results on the equilibrium adsorption of Ba^{2+} by Ca-exchanged montmorillonite fit a Langmuir isotherm (R = 1) of constant K 0.034 mg L^{-1} and maximum adsorption b 15.29 mg g^{-1} (0.22 mequiv. g^{-1}). Eylem et al. [24] indicate parameters of K 0.076 and $1/b$ 3.51×10^{-4} for R^2 = 0.65 from the Langmuir model, even though the authors found that data fitted the Freundlich and Dubinin–Radushkevich equations better; they consider that the kinetics of adsorption is defined by two mechanisms of different first-order rate constants corresponding to adsorption on external sites and on interlayer crystal surfaces [24]. Kleven and Alstad [25] from the $Ba^{2+} \rightarrow Na^{2+}$ exchange on montmorillonite determined adsorption of 0.17–0.24 mequiv./100 g and mean distribution coefficient of 2.7 calculated from linear isotherms (R = 0.999 and 0.960), far below our calculated maximum adsorption of 0.535 mequiv. g^{-1} on Ca-exchanged montmorillonite clay; Kleven and Alstad [25] assumed that lattice substitutions in montmorillonite are responsible for ion exchange additional to montmorillonite's ability to expand its surface area and change the cation exchange capacity; montmorillonite had higher affinity for Ba^{2+} than for Ca^{2+}. Zhang et al. [26] concluded that the adsorption of Ba^{2+} was dependent on surface protonation/deprotonation reactions affected by pH and ionic strength of reactant $NaNO_3$ solution; Ba^{2+} was thought to form inner- and outer-sphere complexes on negatively charged sites of the basal surface and on hydroxyl lateral sites of montmorillonite.

The kinetics of adsorption of Ba^{2+} by Ca-exchanged clinoptilolite tuff which we described by second-order kinetics (R^2 = 0.9999) of rate constant K_v 8.232×10^{-2} g mg^{-1} h^{-1} and maximum adsorption calculated q_e 71.885 mg g^{-1} (1.047 mequiv. g^{-1}) is of the same order that the 1.69 mequiv. g^{-1} (second-order kinetics, K 0.055) recognized for the absorption of Ba^{2+} by NH_4^+-clinoptilolite; the adsorption of Ba^{2+} was second to Pb^{2+} in a series of decreasing efficiency $Pb^{2+} > Ba^{2+} > Cd^{2+}$,$Cu^{2+}$,$Sr^{2+} > Zn^{2+} > Co^{2+}$ [21]. The adsorption of Ba^{2+} by Na-clinoptilolite was found below Pb^{2+}, above Cu^{2+} and of the same order as NH_4^+ in the selectivity series $Pb^{2+} > NH_4^+$, $Ba^{2+} > Cu^{2+}$, $Zn^{2+} > Cd^{2+} > Co^{2+}$ [21]. Our indicated maximum adsorption of Ba^{2+} 1.047 mequiv. g^{-1} is less than the adsorption of Ba^{2+} 0.30 equiv. dm^{-3} (300 mequiv. L^{-1}) by clinoptilolite and 1.0 equiv. dm^{-3} (1000 mequiv. L^{-1}) by Na-clinoptilolite from 0.1N solutions containing variable concentrations of Ba^{2+} and competing cations Cs^{2+}, Sr^{2+}, Pb^{2+}, Ni^{2+} and Cd^{2+}, within selectivity series $Pb^{2+} > Cd^{2+} > Ba^{2+} > Sr^{2+} > Cs^{2+}$ and $Pb^{2+} > Ba^{2+} > Cd^{2+} > Sr^{2+} > Cs^{+} > Ni^{2+}$ for natural and sodium exchange clinoptilolites [22]. Caputo and Pepe [1] reviewed the adsorption studies on Italian zeolites to conclude that Na-exchanged phillipsite and chabazite but not clinoptilolite can successfully adsorb Ba^{2+}.

4. Conclusions

Kinetics and equilibrium adsorption of Ba^{2+} by Ca-exchanged clinoptilolite tuff and Ca-exchanged montmorillonite clay are first presented. The Ba^{2+} uptake from 0.1N $BaCl_2$ solution is described by second-order kinetics (R^2 = 0.999) of rate constant K_v of 8.232×10^{-2} g mg^{-1} h^{-1} and calculated adsorption of 71.885 mg g^{-1}. Adsorption comprises an initial stage where Ba^{2+} is adsorbed at a high rate and a second stage whereby more moderate adsorption develops. The equilibrium uptake of Ba^{2+} from $BaCl_2$ + $CaCl_2$ solution of variable concentration 0.1 to 0.005N,

Ba^{2+}/Ca^{2+} ratio 1, is described by a Langmuir adsorption isotherm ($R = 1$) of maximum Ba^{2+} adsorption 15.29 mg g^{-1} and constant K 0.015 L mg^1. The absorption kinetics of Ba^{2+} by Ca-exchanged montmorillonite is defined by a second-order reaction ($R^2 = 0.999$) of constant K_v 3.179×10^{-2} g mg^{-1} h^{-1} and calculated absorption q_e 36.743 mg g^{-1}. Adsorption follows the Langmuir model defined by the equilibrium constant K 0.034 L mg^{-1} and a maximum adsorption of 15.29 mg g^{-1}.

Acknowledgements

The present work was financed through Project P47075000 of the Consejo Nacional de Ciencia y Tecnologia CONACYT, The authors are indebted to M.C Salcedo, A. Tovar, M. Gutiérrez, M. Portillo, E.S. Reynoso, B. Gómez, A. Huerta, K. Shimada, M. Abatal and R. Ibarra for their collaboration.

References

[1] D. Caputo, F. Pepe, Experiments and data processing of ion exchange equilibria involving Italian natural zeolites: a review, Micropor. Mesopor. Mater. 105 (2007) 222–231.
[2] S.S. Gupta, K.G. Bhattacharyya, Immobilization of Pb(II), Cd(II) and Ni(II) ions on kaolinite and montmorillonite surfaces from aqueous medium, J. Environ. Manage. 87 (2008) 46–58.
[3] K.G. Bhattacharyya, S.S. Gupta, Influence of acid activation on adsorption of Ni(II) and Cu(II) on kaolinite and montmorillonite: kinetic and thermodynamic study, Chem. Eng. J. 136 (2008) 1–13.
[4] K. Gedik, I. Imamoglu, Removal of cadmium from aqueous solutions using clinoptilolite: influence of pretreatment and regeneration, J. Hazard. Mater. 155 (2008) 385–392.
[5] R. van Herwijnen, T.R. Hutchings, A. Al-Tabbaa, A.J. Moffat, M.L. Johns, S.K. Ouki, Remediation of metal contaminated soil with mineral-amended composts, Environ. Pollut. 150 (2007) 347–354.
[6] V.J. Inglezakis, M.A. Stylianou, D. Gkantzou, M.D. Loizidou, Removal of Pb(II) from aqueous solutions by using clinoptilolite and bentonite as adsorbents, Desalination 210 (2007) 248–256.
[7] N.W. Ockwig, R.T. Cygan, L.J. Criscenti, T.M. Nwnoff, Molecular dynamics studies of nanoconfined water in clinoptilolite and heulandite zeolites, Phys. Chem. Chem. Phys. 10 (2008) 800–807.
[8] M. Sprynskyy, B. Buszewski, A.P. Terzyk, J. Namiesnik, Study of the selection mechanism of heavy metal (Pb^{2+}, Cu^{2+}, Ni^{2+} and Cd^{2+}) adsorption on clinoptilolite, J. Colloid Interface Sci. 304 (2006) 21–28.
[9] M. Sprynskyy, Solid–liquid–solid extraction of heavy metals (Cr, Cu, Cd, Ni and Pb) in aqueous systems of zeolite–sewage sludge, J. Hazard. Mater. 161 (2009) 1377–1383.
[10] S.C. Stefanovic, N.Z. Logar, K. Margeta, N.N. Tusar, I. Arcon, K. Maver, J. Kovac, V. Kaucic, Structural investigation of Zn^{2+} sorption on clinoptilolite tuff from the Vranjska Banja deposit in Serbia, Micropor. Mesopor. Mater. 105 (2007) 251–259.
[11] M.A. Stylianou, V.J. Inglezakis, K.G. Moustakas, S.P. Malamis, M.D. Loizidou, Removal of Cu(II) in fixed bed and batch reactors using natural zeolite and exfoliated vermiculite as adsorbents, Desalination 215 (2007) 133–142.
[12] A. Dimirkou, Uptake of Zn^{2+} ions by a fully iron-exchanged clinoptilolite. Case study of heavily contaminated drinking water samples, Water Res. 41 (2007) 2763–2773.
[13] S. Kocaoba, Y. Orhan, T. Akyüz, Kinetics and equilibrium studies of heavy metal ions removal by use of natural zeolite, Desalination 214 (2007) 1–10.
[14] P. Kosobucki, M. Kruk, B. Buszewski, Immobilization of selected heavy metals in sewage sludge by natural zeolites, Bioresour. Technol. 99 (2008) 5972–5976.
[15] M.E. Argun, Use of clinoptilolite for the removal of nickel ions from water: kinetics and thermodynamics, J. Hazard. Mater. 150 (2008) 587–595.
[16] S. Coruh, The removal of zinc ions by natural and conditioned clinoptilolites, Desalination 225 (2008) 41–57.
[17] P. Boulet, H.C. Greenwell, S. Stackhouse, P.V. Coveney, Recent advances in understanding the structure and reactivity of clays using electronic structure calculations, J. Mol. Struct. Theochem 762 (2006) 33–48.
[18] S.S. Gupta, K.G. Bhattacharyya, Removal of Cd(II) from aqueous solution by kaolinite, montmorillonite and their poly(oxo zirconium) and tetrabutylammonium derivatives, J. Hazard. Mater. B128 (2006) 247–257.
[19] K.G. Bhattacharyya, S.S. Gupta, Adsorptive accumulation of Cd(II), Co(II), Cu(II), Pb(II), and Ni(II) from water on montmorillonite: influence of acid activation, J. Colloid Interface Sci. 310 (2007) 411–424.
[20] B. De Gennaro, P. Aprea, C. Colella, A. Buondonno, Comparative ion-exchange characterization of zeolitic and clayey materials for pedotechnical applications—Part 1: Interaction with noxious cations, J. Porous Mater. 14 (2007) 349–356.
[21] G. Blanchard, M. Maunaye, G. Martin, Removal of heavy metals from waters by means of natural zeolites, Water Res. 18 (1984) 1501–1507.
[22] H. Faghihian, M.G. Marageh, H. Kazemian, The use of clinoptilolite and its sodium form for removal of radioactive cesium, and strontium from nuclear wastewater and Pb^{2+}, Ni^{2+}, Cd^{2+}, Ba^{2+} from municipal wastewater, Appl. Radiat. Isot. 50 (1999) 655–660.
[23] B. de Gennaro, A. Colella, P. Aprea, C. Colella, Evaluation of an intermediate-silica sedimentary chabazite as exchanger for potentially radioactive cations, Micropor. Mesopor. Mater. 61 (2003) 159–165.
[24] C. Eylem, H.N. Erten, H. Göktürk, Sorption–desorption behaviour of barium on clays, J. Environ. Radioact. 11 (1990) 183–200.
[25] R. Kleven, J. Alstad, Interaction of alkali, alkaline-earth and sulphate ions with clay minerals and sedimentary rocks, J. Petrol. Sci. Eng. 15 (1996) 181–200.
[26] P.-C. Zhang, P.V. Brady, S.E. Arthur, W.-Q. Zhou, D. Sawyer, D.A. Hesterberg, Adsorption of barium (II) on montmorillonite: an EXAFS study, Colloids Surf. A: Physicochem. Eng. Aspects 190 (2001) 239–249.
[27] J.G. Atun, E. Bascetin, Adsorption of barium on kaolinite, illite and montmorillonite at various ionic strengths, Radiochim. Acta 91 (2004) 223–228.
[28] S. Van Roy, K. Vanbroekhoven, W. Dejonghe, L. Diels, Immobilization of heavy metals in the saturated zone by sorption and in situ bioprecipitation processes, Hydrometallurgy 83 (2006) 195–203.
[29] C. Madoz-Escande, O. Simon, Contamination of terrestrial gastropods, Helix aspersa maxima, with ^{137}Cs, ^{85}Sr, ^{133}Ba and ^{123m}Te by direct, trophic and combined pathways, J. Environ. Radioact. 89 (2006) 30–47.
[30] J. Al-Jundi, E. Al-Tarazi, Radioactivity and elemental analysis in the Ruseifa municipal landfill, Jordan, J. Environ. Radioact. 99 (2008) 190–198.
[31] J.M. Neff, Estimation of bioavailability of metals from drilling mud barite, Integr. Environ. Assess. Manage. 4 (2008) 184–193.
[32] A. González, G. Cuevas, C. Vélez, D. Hernández, Caracterización de suelos y evaluación del contenido de metales pesados en zonas urbanas del Estado de Chihuahua, Memorias del Congreso Nacional "Participación de la Sociedad en los Retos Ambientales". Realizado del 12 al 14 de Mayo de 2004, en Mazatlán, Sinaloa. XIV Congreso Nacional de Ingeniería Sanitaria y Ambiental.
[33] S. Franciskovic-Bilinski, Barium anomaly in Kupa River drainage basin, J. Geochem. Explor. 88 (2006) 106–109.
[34] M. Shuhaimi-Othman, I. Mushrifah, E.C. Lim, A. Ahmad, Trend in metals variation in Tasik Chini, Pahang, Peninsular Malaysia, Environ. Monit. Assess. 143 (2008) 345–354.
[35] Y. Shinkai, D.V. Truc, D. Sumi, D. Canh, Y. Kumagai, Arsenic and other metal contamination of groundwater in the Mekong River Delta, Vietnam, J. Health Sci. 53 (2007) 344–346.
[36] F. Baldi, M. Pepi, D. Burrini, G. Kniewald, D. Scali, E. Lanciotti, Dissolution of barium from barite in sewage sludges and cultures of Desulfovibrio desulfuricans, Appl. Environ. Microbiol. 62 (1996) 2398–2404.
[37] D. Meza-Figueroa, M. De la O-Villanueva, M.L. De la Parra, Heavy metal distribution in dust from elementary schools in Hermosillo, Sonora, México, Atmos. Environ. 41 (2007) 276–288.
[38] U. S. Environmental Protection Agency, EPA: http://www.epa.gov/safewater/agua/estandares.html.
[39] M. Purdey, Chronic barium intoxication disrupts sulphated proteoglycan synthesis: a hypothesis for the origins of multiple sclerosis, Med. Hypotheses 62 (2004) 746–754.
[40] N.J.G. Pearce, V.L. Mann, Trace metal variations in the shells of Ensis siliqua record pollution and environmental conditions in the sea to the west of mainland Britain, Mar. Pollut. Bull. 52 (2006) 739–755.
[41] D.-Y. Wang, Y. Wang, Phenotypic, Behavioral defects caused by barium exposure in nematode Caenorhabditis elegans, Arch. Environ. Contam. Toxicol. 54 (2008) 447–453.
[42] S.R. Oliva, B. Valdés, M.D. Mingorance, Evaluation of some pollutant levels in bitter orange trees: implications for human health, Food Chem. Toxicol. 46 (2008) 65–72.
[43] L. de Pablo-Galán, Geochemical trends in the alteration of Miocene vitric tuff to economic zeolite deposits, Oaxaca, Mexico, Appl. Geochem. 1 (1986) 273–285.
[44] L. de Pablo-Galán, M.L. Chávez-García, G. Dimas, Diagenesis of Miocene vitric tuffs to zeolites, Mexican Highlands, Mexico, Miner. Mag. 58A (1994) 682–683.
[45] L. de Pablo-Galán, Diagenesis of Oligocene-Miocene vitric tuffs to montmorillonite and K-feldspar deposits, Durango, Mexico, Clays Clay Miner. 38 (1990) 426–436.
[46] L. de Pablo-Galán, J.J. de Pablo, M.L. Chávez-García, Diagenesis and shear rheology of a Recent-Pleistocene volcanogenic sequence, Mexican Basin. Implications and swelling and stability, Rev. Mex. Ciencias Geol. 18 (2001) 175–185.
[47] S. Enciso, Hoja Cuencamé: Instituto de Geología, Universidad Nacional A. de México City, Mexico, map, 1968.
[48] I. Ferrusquilla, Contribución al conocimiento geológico de Oaxaca, México –El área Laollaga-Lachiviza. Universidad Nacional Autónoma de México, Instituto de Geología, Boletín No. 110, 1999.
[49] F.A. Mumpton, First reported occurrence of zeolites in sedimentary rocks of Mexico, Am. Miner. 58 (1973) 287–290.
[50] C. Schlaepfer, L. de Pablo, Mineralogia de las arcillas rojas de Oaxaca, Boletín Sociedad Mexicana Geologos Petroleros XXVII (1964) 93–117.
[51] Y.S. Ho, J.C.Y. Ng, G. McKay, Removal of lead (II) from effluents by sorption on peat using second-order kinetics, Sep. Sci. Technol. 36 (2001) 241–246.
[52] R.T. Pabalan, F.P. Bertetti, Cation-exchange properties of natural zeolites, in: D. Bish, D. Ming (Eds.), Natural Zeolites: Occurrence, Properties, Applications, vol. 45, Rev. Mineral. Geochem. Mineralogical Society of America, Washington, 2001, pp. 453–464.
[53] J.M. Cases, I. Bérend, M. Francois, J.R. Uriot, L.J. Michot, E. Thomas, Mechanisms of adsorption and desorption water vapor by homoiónica montmorillonite: 3.

The Mg^{2+}, Ca^{2+}, Sr^{2+} and Ba^{2+} exchanged forms, Clays Clay Miner. 45 (1997) 8–22.
[54] P. Castaldi, L. Santona, C. Cozza, V. Giuliano, C. Abbruzzese, V. Nastro, P. Melis, Thermal and spectroscopic studies of zeolites exchanged, J. Mol. Struct. 734 (2005) 99–105.
[55] E.R. Nightingale, Phenomenological theory of ion solvation. Effective radii of hydrated ions, J. Phys. Chem. 63 (1959) 1382–1387.
[56] S.E. Rodríguez-Cruz, R.A. Jockusch, E.R. Williams, Hydration energies and structures of alkaline earth metal ions, $M^{2+}(H_2O)_n$, $n = 5–7$, M = Mg, Ca, Sr, and Ba, J. Am. Chem. Soc. 121 (1999) 8898–8906.